The Meteoritical Society

Meteoritics & Planetary Science 49, Nr 12, 2152–2168 (2014)
doi: 10.1111/maps.12381

Revisiting the Rochechouart impact structure, France

Haley M. SAPERS[1,2*], Gordon R. OSINSKI[1,3], Neil R. BANERJEE[1], Ludovic FERRIÈRE[1,4], Philippe LAMBERT[5], and Matthew R. M. IZAWA[1,6]

[1]Department of Earth Sciences and the Centre for Planetary Science and Exploration, Western University, 1151 Richmond Street, London, ON N6A 5B7, Canada
[2]Department of Natural Resource Science, McGill Université, Macdonald Campus, 21,111 Lakeshore Road St. Anne de Bellevue, Québec H9X 3V9, Canada
[3]Department of Physics & Astronomy, University of Western Ontario, 1151 Richmond Street, London, Ontario N6A 5B7, Canada
[4]Natural History Museum, Burgring 7, A-1010 Vienna, Austria
[5]Sciences et Applications, 218 Boulevard Albert 1er, 33800 Bordeaux, France
[6]Department of Geography, University of Winnipeg, 515 Portage Avenue, Winnipeg, Manitoba R3B 2E9, Canada
*Corresponding author. E-mail: haley.sapers@gmail.com

(Received 08 January 2014; revision accepted 19 July 2014)

Abstract–The Rochechouart impact structure, south-central France (45°50′N, 0°46′E), is a partly eroded, approximately 200 Myr, complex impact structure. The impactite suite at Rochechouart provides an excellent example of gradational boundaries and transitional lithologies that have been historically difficult to classify with standard impactite nomenclature. Here, we present the first detailed scanning electron microscopy-based description of the Rochechouart impactites integrated with hand-sample and petrographic observations with the goal of understanding the clast-matrix relationships of transitional lithologies. Three main impact-generated hydrothermal alteration assemblages are also recognized: (1) argillic-like, (2) carbonate, and (3) oxide. Our results support the existence of a continuum between clast-rich impact melt rocks and glass-rich clastic breccias (suevites) that must be represented in universal classification schemes. This suite of impactites from the Rochechouart impact structure is used as a test case for a recently published classification scheme based on the nature of the groundmass setting a precedent for classification of impactites with limited to no geological context such as deeply eroded terrestrial impact structures and future sample return missions. The re-evaluation of the melt-bearing Rochechouart impactites questions the currently accepted size of the crater, suggesting a much larger original crater diameter.

INTRODUCTION

Impact cratering is one of the most important geological processes on the terrestrial planets and rocky and icy moons of the solar system. It has become increasingly apparent over the past two decades that impact cratering has played a major role in shaping the origin and evolution of Earth, and possibly of life itself. Classification of the lithological products of impact cratering has been the subject of much recent debate. Impactites comprise all rocks affected by impact processes and range from fractured, displaced, and/or shocked rocks (including shatter cones) and lithic (melt-free) breccias, to impact melt-bearing breccias, melt rocks, and tektites (Stöffler and Grieve 2007). Currently extant classification schemes do not account for intermediate lithologies and, as a result, transitional lithologies are inadequately described by endmember nomenclature. Further to the issue of transitional lithologies, the currently accepted IUGS impactite classification scheme is based on the location of the impactite with respect to the transient cavity to infer a mode of occurrence (Stöffler and Grieve 2007). Such classification requires interpretation of field context and absolute knowledge of the location of the crater rim. Both of these requirements are often difficult to determine leading to ambiguous and inconsistent use of nomenclature.

The Rochechouart impact structure is an eroded, late Triassic impact site, located in south-central France (45°50′N and 0°46′E; Kraut et al. 1969; Kraut and French 1971). Despite erosion, a wide variety of impactites are preserved. The petrographic evaluation of the Rochechouart impactites presented here allows for a systematic classification integrating the most recent recommendations of the IUGS Subcommission on the Systematics of Metamorphic Rocks (SCMR) with descriptive nomenclature allowing for indeterminate and transitional units. Such a classification system based on observable, intrinsic characteristics can be extrapolated to collections where there is an extremely limited sample size or complete lack of field context such as deeply eroded impact structures, drill cores, Apollo samples, meteorites, and future planetary sample returns. Being able to correlate these samples and compare them to samples with a field context is invaluable and fundamental to understanding impact cratering as a geological process occurring not just on Earth but also on other terrestrial bodies. While detailed petrographic studies at the thin-section to hand-sample scale have been conducted on Rochechouart impactites (e.g., Kraut and French 1971; Lambert 1974, 1977c), the complex relationships between clasts and matrix as well as the nature of the matrix itself can only be fully observed at the micrometer to nanometer scale using scanning electron microscopy (SEM) imaging techniques (e.g., Nelson et al. 2012; Osinski and Spray 2001; Osinski et al. 2004). We have carried out such a study for the first time on Rochechouart impactites. This detailed high-resolution study of the Rochechouart impactites not only has implications for the crater size and its formation, but, furthermore, this study sets a precedent for the classification of indeterminate lithologies that do not fit the endmember nomenclature, as well as in situations where field context is unavailable.

GEOLOGICAL SETTING OF THE ROCHECHOUART IMPACT STRUCTURE

The Rochechouart impact structure was formed in dominantly (approximately 300–400 Myr) granitic intrusive and metamorphic rocks containing subordinate Neoproterozoic intrusives at the northwestern edge of the French Massif Central near the margin of a Mesozoic sea (e.g., Reimold and Oskierski 1987; Turpin et al. 1990). The crystalline target rocks are comprised of granite; gneiss; and metamorphosed, intercalated, fine-grained quartzofeldspathic and metabasic rocks (leptynites) of the Massif Central (Turpin et al. 1990). The crystalline basement is unconformably overlain to the west by the Triassic–Cretaceous limestones and other sedimentary strata of the Aquitaine Basin (Lambert 1977c). The currently most-accepted age of the Rochechouart structure, 214 $\pm$ 8 Ma, is based on $^{40}Ar/^{39}Ar$ laser spot fusion dating of pseudotachylite generated during transient crater collapse (Kelley and Spray 1997). However, recent age determinations on potassium-feldspar in shocked gneisses generated during K-metasomatism as a result of postimpact hydrothermal activity suggest an age of 202.7 $\pm$ 2.2 Ma (2σ; recalculated by Schmieder [personal communication] from Schmieder et al. [2010] using the revised K decay constants of Renne et al. [2010, 2011]; see Jourdan et al. [2012]), coincident within error of the Triassic–Jurassic boundary (currently reported at an age of 201.3 $\pm$ 0.2 Ma in the latest international chronostratigraphic chart; Cohen et al. 2013). A direct age relationship between the Rochechouart impact event and the Triassic–Jurassic boundary, however, can only be established with more precise and accurate age data for both the impact and extinction event. The younger age for the structure reported by Schmieder is suggested as being a more robust age, as the pseudotachylite dating may have suffered from an extraneous argon component likely resulting from the incomplete degassing of inherited clasts during friction melting (Schmieder et al. 2010). There is no evidence of hydrothermal activity in the region capable of generating K-feldspar subsequent to the impact event, yielding the 202.7 $\pm$ 2.2 Ma date as the currently most robust age for the Rochechouart structure.

As a result of erosion, the Rochechouart impact structure is not delimited by any specific topographic expression, as previously described by Kraut and French (1971; Fig. 1). Originally interpreted as a volcanic feature, the identification of shock metamorphic features such as planar deformation features (PDFs) in quartz (Kraut 1967) and shatter cones (Kraut 1969; Kraut et al. 1969) led to the recognition of an impact origin. Rochechouart contains scattered outcrops of monomict and polymict impact breccias, impact melt-bearing rocks, shatter cones, and other shocked target rocks (e.g., Lambert [2010] and references therein). Allochthonous impactites (impact breccias and impact melt-bearing materials) occur as remnant outcrops distributed in a centrosymmetric, discontinuous sheet, over an area of approximately 150 km^2 (Fig. 1). These outcrops delineate a somewhat circular area with a diameter of approximately 15 km that was considered by Kraut and French (1971) to be "the minimum original diameter of the crater." Estimating the original crater size is an area of active debate (e.g., Lambert 1974, 1977c, 2010). Pohl et al.

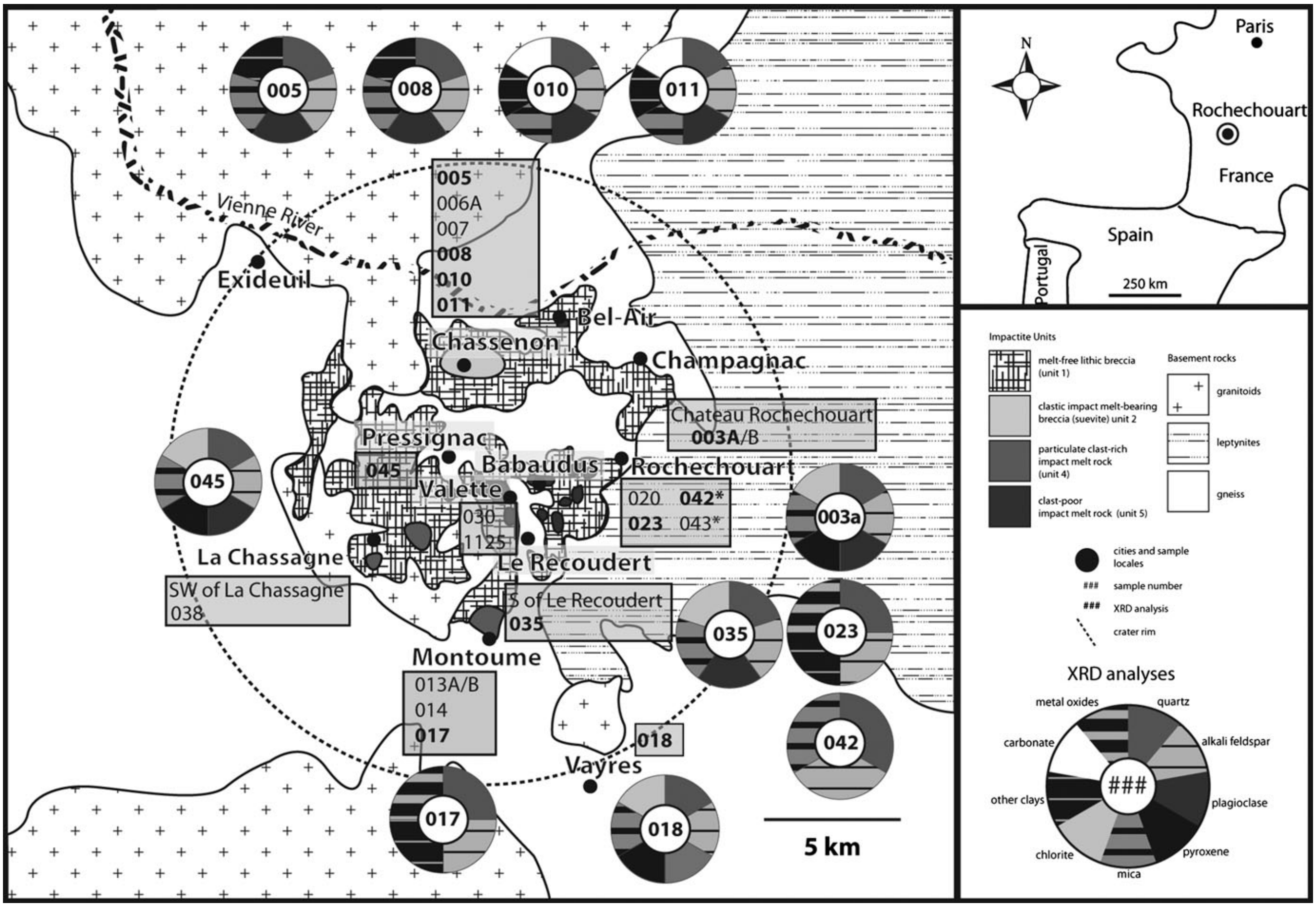

Fig. 1. Simplified geologic map of the Rochechouart impact structure, with sample locations; modified from Kelley and Spray (1997), and Lambert (1974, 1977c). The dotted line delineates the 23 km impact structure. Mineralogy for selected samples based on bulk XRD analysis is illustrated by the pie charts (see text for details). Note that the wedge size is not indicative of relative mineral amounts, but rather the presence of a particular mineral phase. Basement samples: 010, 018, 038, 045; unit 1, melt-free lithic impact breccia (Rochechouart breccia): 003, 020, 023, 035; unit 2, clastic impact melt-bearing lithic breccia (Chassenon suevite): 005, 006, 011; unit 3, melt-rich impactite (basal suevite or Valette-type breccias): 1123; unit 4, particulate, clast-rich impact melt rock (Montoume breccia): 008, 013, 014, 017, 029, 030; unit 5, impact melt rock (Babaudus melt): 042, 043.

(1978) cite a diameter related to the 18–25 km diameter disturbed zone, which represents the minimum diameter of the structure. This estimate is consistent with a negative gravity anomaly centered on the structure (Pohl et al. 1978). A shock zoning study conducted by Lambert (1977c) estimated the size of the structure to be 20–25 km. Recently, a 40–50 km diameter for the size of the initial crater at Rochechouart has been proposed (Lambert 2010). The conservative estimates (18–25 km) are based on the extent of damage to the basement and do not take into account the extensive removal of material by erosion.

The impact structure has been affected by later regional tectonic activity (Kraut and French 1971). A north–south cross sectional profile indicates that regional deformation has tilted the crater floor about 0.6^{o} to the north such that the southern part of the structure is raised relative to the northern region (Lambert 1977a, 2010). It is notable that the structural crater floor beneath the allochthonous impactites is extremely flat, ± 50 m over 300 km^2 (Lambert 1977a, 1982, 2010).

The Rochechouart allochthonous impactites are complex and heterogeneous at all scales. Five main impactite units overlying the impact-damaged parautochthonous basement rock have been described as follows with many of the units named with respect to their location of discovery and/or main occurrence (Fig. 2; Table 1): unit 1) lithic breccia ("Rochechouart breccia"); unit 2) suevitic breccia ("Chassenon suevite"); unit 3) "basal suevite," a recently discovered transitional impact melt-bearing breccia (see Lambert 2010); unit 4) red "welded" breccia or "suevite" ("Montoume breccia"); unit 5) finely crystalline melt rock ("Babaudus

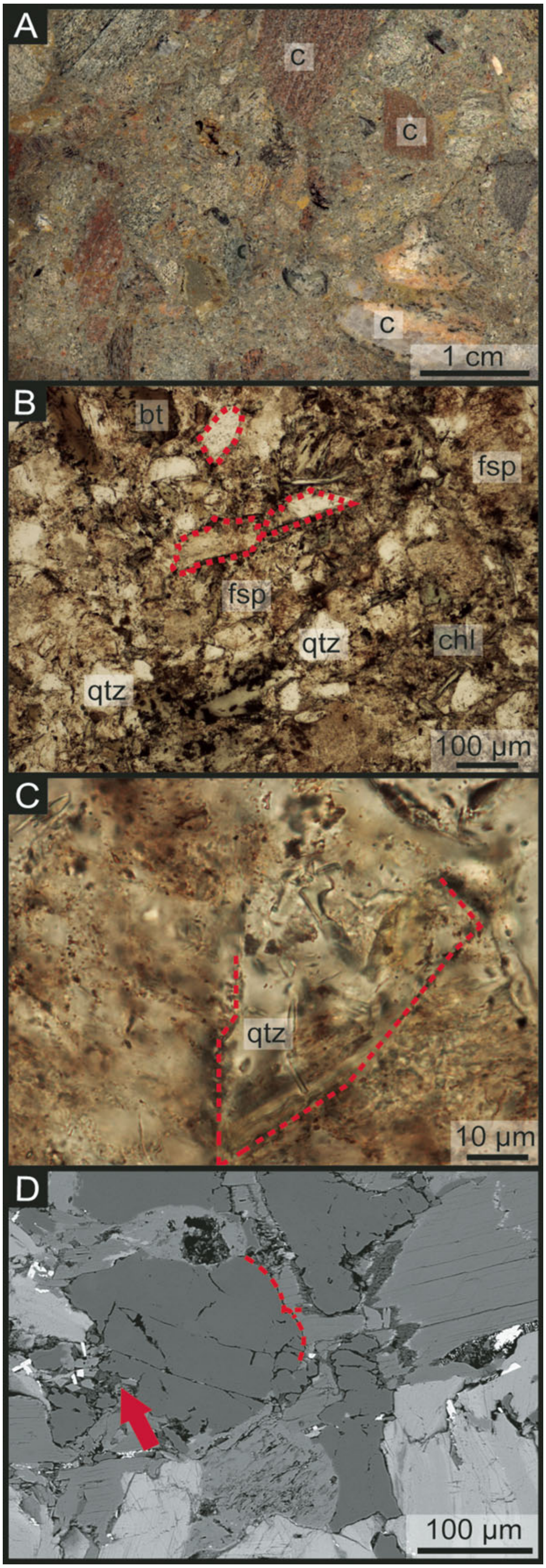

Fig. 2. Unit 1: lithic impact breccia (Rochechouart breccia, from Rochechouart). A) Hand sample. Note the clastic nature of the sample composed of various fragmented lithic clasts (c). There is a notable absence of melt/glassy inclusions. B–C) Transmitted light micrographs: Note the clastic nature of the groundmass composed of various lithic and mineral clasts (bt = biotite; qtz = quartz; fsp = feldspar). Sharp, irregular grain boundaries are outlined. Chloritization (chl) is also observed. D) Backscattered electron (BSE) image. Note the fragmental, cataclastic nature of the groundmass and the similarity of the jagged, sharp grain boundaries (outlined) to those in the melt-bearing impact breccia. Also note the fine-grained clastic matrix material between larger clasts (arrow).

melt;" Kraut and French 1971). Lambert (1974, 1977b, 1977c) described and named the Rochechouart impactites based on shock level, in contrast with the stratigraphic ordering of Kraut and French (1971). It is noted that Kraut (1969) and Kraut and French (1971) described the lithologies generated by impacts corresponding to their informal locality-based nomenclature. In the present study, we have followed and expanded upon Lambert's (1974) original classification. For clarity and consistency, in this paper we will refer to the different impactites as unit 1, 2, etc., in the results section. We then reclassify and reinterpret these impactites in the discussion section.

METHODOLOGY

Twelve samples representing each of the five main impactite lithologies described above were prepared for powder X-ray diffraction (XRD) analysis. X-ray diffraction data were collected from 2^o to 82^o 2θ with a step size of 0.02^o and scanning speed of 10^o per min using a Rigaku Rotaflex diffractometer operating at 45 kV and 160 mA with a Co rotating anode source (Co $K\alpha$, $\lambda = 1.7902$ Å). Diffractograms were analyzed using the BrukerAXS EVA software package (BrukerAXS, 2005) and the International Center for Diffraction Data (ICDD) PDF-4 database. Nineteen representative polished thin sections from sixteen samples representing each of the main impact lithologies were chosen for petrographic study in transmitted light. Polished, carbon-coated thin sections were analyzed using a Hitachi S-4300S/E field emission variable pressure scanning electron microscope with EDAX Pegasus 4040 integrated EDX/EBSD X-ray spectrometer at the Imaging Center, Texas Tech University (Lubbock, Texas, USA); with 15 kV accelerating voltage, and a working distance approximately 12–15 mm. Backscattered electron (BSE) and secondary electron (SE) imaging was also carried out using a tungsten-filament Hitachi S-2500C SEM at the Zircon and

Table 1. Summary of nomenclature used to describe the Rochechouart impactites.

	This Study	Lambert (2010)	Lambert (1977a, 1977b, 1977c)	Kraut (1969)
n.a.	Shocked/fractured basement	Shocked basement	A (fractured basement rock)	n.a.
n.a.	Monomict lithic breccia	Monomict lithic breccia	B (monomict breccia)	Rochechouart breccia
Unit 1	Lithic impact breccia	Polymict lithic breccia	C (polymict breccia, no glass)	
Unit 2	Melt-bearing impact breccia	Melt-poor suevite	D (polymict breccia, with glass)	Chassenon suevite
Unit 3	Melt-rich impactite	Melt-rich (basal) suevite	n.a.	n.a.
Unit 4	Particulate impact melt rock	Impact melt	E (melt)	Montoume breccia
Unit 5	Impact melt rock			Babaudus melt

n.a. = not applicable to the referenced study.
Units are ordered by increasing content of impact melt.

Accessory Phase Laboratory, University of Western Ontario. Additional high-resolution BSE imaging and EDX spot analysis was carried out with a Leo 1540 FIB/SEM CrossBeam field emission SEM equipped with an Oxford Instruments INCA EDX system allowing for semiquantitative elemental analysis, sensitive to approximately 0.5 wt% or less for all elements from C–U in the Nanofabrication Laboratory, University of Western Ontario. The sections were analyzed under high vacuum with an accelerating voltage of 15–20 kV and a working distance approximately 10 mm. Energy dispersive X-ray (EDX) spectroscopy mapping and spot analyses of selected samples allowed for the identification of mineral phases that are present in low concentrations beneath the bulk XRD threshold.

RESULTS

Petrographic Shock Indicators

All impactites examined contain petrographic indicators of shock metamorphism, including planar fractures (PF) and planar deformation features (PDFs) in quartz, mosaicism of quartz, diaplectic quartz glass, and feldspar glass. Kink banding in mica was also observed in many of the investigated samples; even though kink banding is not considered to be an unambiguous indicator of shock metamorphism, it is clear that in the present case, kink banding is related to the impact event. The presence of "toasted quartz" (e.g., Ferrière et al. 2009b; Whitehead et al. 2002) was also noted in all of the melt-bearing impactite lithologies. Ballen silica was observed in "Babaudus melt" and in "Montoume breccia" samples, in agreement with previous reports by Ferrière et al. (2009a, 2010). The petrographic shock indicators observed in this study are consistent with previous studies (e.g., Lambert 1977c) indicating that clasts within both the autochthonous and the allochthonous impactites have been subjected to a range of shock pressures and postshock temperatures.

Bulk Mineralogy

Bulk powder XRD was used to determine the major minerals present in each of the impactite units, as well as in the unshocked basement rocks (Fig. 1). As expected from the crater-scale geologic setting, the mineralogy is somewhat limited and consistent with the Hercynian target rocks. Diffractograms containing peaks corresponding to clay minerals, calcite, and Fe-Ti-oxides are also suggestive of various alteration phases. Phyllosilicates including muscovite, glauconite, illite, chlorite, and montmorillonite/smectite group clays, were identified by XRD in all units, including the unshocked basement rocks. Analyses from the units 1 and 4 have XRD patterns corresponding to Fe-Ti-oxides (hematite, ilmenite, and lepidocrocite). Bulk XRD analysis of an altered glass clast from unit 2 indicated quartzofeldspathic mineralogy consistent with the bulk impactite. However, alteration mineralization (calcite and mica-clay minerals) is more prevalent in the glass clast compared to the bulk impactite.

Groundmass Textures and Clasts

Unit 1: ("Rochechouart Breccia")

Transmitted light microscopy observations indicate that the groundmass is composed of angular to subangular lithic and mineral fragments of quartzofeldspathic composition set in a matrix of fine-grained material, forming a cataclastic texture (Fig. 2). The fine-grained matrix is a minor component compared to the lithic and mineral clasts (Fig. 2B). Mineral and lithic fragments range in size from approximately 2–15 μm to larger clasts of up to a centimeter in size. However, at hand sample and outcrop scale (e.g., impact breccia-derived building stone of Rochechouart Castle), clasts are observed up to several decimeters in size. Mineral clasts are dominantly feldspars, mica, and quartz. Mineral grains display various shock-induced features including fracturing, PDFs in quartz, and partial melting. Chloritization is present (Fig. 2B) and is pervasive in some areas giving the matrix a "crystalline" appearance. No impact glass clasts were observed in the investigated samples.

Backscattered electron images highlight the angular clastic matrix of the polymict lithic breccia (Fig. 2D). Mineral grains have discrete margins, are fragmented, and fractured, and range in size from >1 μm to >500 μm. Most mineral grains have angular to subangular boundaries. Rare rounded apatite grains were also observed. Evidence of variable shock levels in mineral clasts was observed, including kink banding in mica, fracturing, and displacement of mineral grains. Some quartz grains show evidence of partial melting. Spaces between large mineral and lithic clasts are infilled by fine-grained clastic material (Figs. 2C and 2D). Uncommon, submicron Fe-Ti oxide grains disseminated in the matrix were also observed (Fig. 2D).

Unit 2: ("Chassenon Suevite")

Transmitted light microscopy suggests that the groundmass is composed of angular to subangular lithic and mineral fragments in a matrix of fine-grained material forming a cataclastic texture (Fig. 3). Mineral fragments are generally smaller than those observed in unit 1, ranging in size from approximately 2–5 μm (Fig. 3C). In contrast to the unit 1, the matrix material of unit 2 is a major component forming approximately 50% of the bulk rock (Fig. 3B). Mineral clasts are dominantly feldspar, mica, and quartz. Shock-induced features are observed including irregular fracturing, PDFs in quartz, and partial melting (Figs. 3B and 3C). Impact glass clasts are present and are irregular in shape with ameboid margins and vary in size from micrometers to centimeters (Figs. 3B and 3C). There is a diversity of glass clasts observed. The color of the glass ranges from black through pale green to locally an intense green and bluish-green. In some samples the glass has been altered

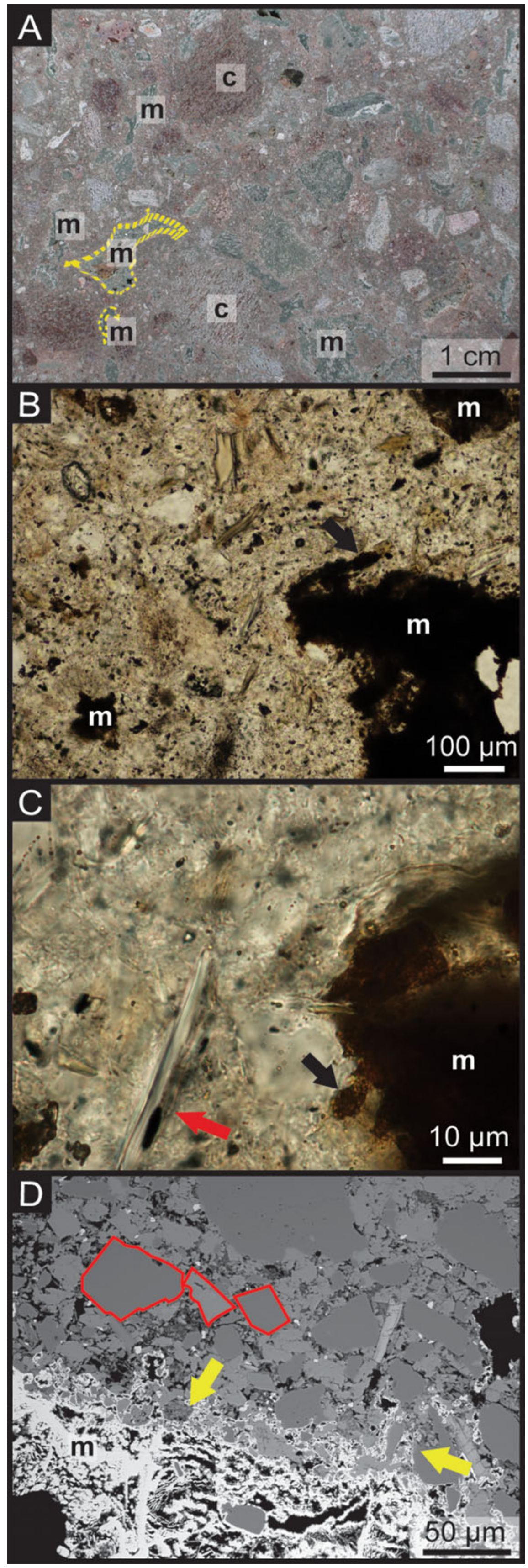

Fig. 3. Unit 2: melt-bearing impact breccia (Chassenon suevite, from Chassenon). A): Hand sample. Note the numerous lithic clasts (c) and melt inclusions (m). Melt inclusions have complex, delicate, ameboid morphologies (dashed line) unlikely to survive aerial transport suggesting "ignimbrite-type" deposition and emplacement as a ground-hugging surge flow. B–C): Transmitted light photomicrographs. Note the clastic nature of the matrix (arrow). Former melt clasts (m) have irregular borders and have recrystallized to a red-brown mineral phase. Note the irregular ameboid protrusions of the former melt inundating the clastic matrix (black arrows). D) Backscattered electron (BSE) image. Note the fragmental, cataclastic nature of the groundmass (example grains outlined). The melt phase has recrystallized to a Fe-Ti oxide (white phase at bottom of image). Notice the former melt inundating the grains of the matrix forming an interstitial phase (arrows).

to a deep red-brown material. All glassy clasts have intricate relationships with the matrix (Fig. 3C).

SEM observations of the matrix are very similar to unit 1, comprising fragmental, angular mineral grains (Fig. 3D) displaying various shock-induced features, including fractures and annealed PDFs in quartz. Areas of formerly glassy melt inclusions are now replaced with Fe-Ti oxides similar in composition to the Fe-Ti oxide grains present in unit 1 (Fig. 3D), probably a mixture of (titano) magnetite and ilmenite. Occasionally, flow banding is preserved by the orientations of the oxide grains. Euhedral Fe-Ti oxide crystals have replaced the primary margin between fine-grained matrix breccia and altered melt (Fig. 3D). The fine-grained infilling breccia contains euhedral to subhedral feldspar crystals at the interface between altered melt and matrix.

Unit 3: ("Basal Suevite")

The impact glass (altered and fresh) and melt domain content of this unit (also known as Valette-type breccias) visible in hand specimen varies from <10% to >60%. Numerous lithic clasts, angular to rounded, and of varying shock level are present. Some of these clasts are enclosed by glass (Fig. 4A). The matrix is purple in color while that of the glass fragments varies from deep red to yellow. The glass and matrix boundaries are irregular in shape and convoluted. In plane-polarized light the intricate textures between the matrix and melt are easily observed (Fig. 4B). Red-brown, micrometer-scale, irregularly shaped grains (probably Fe-

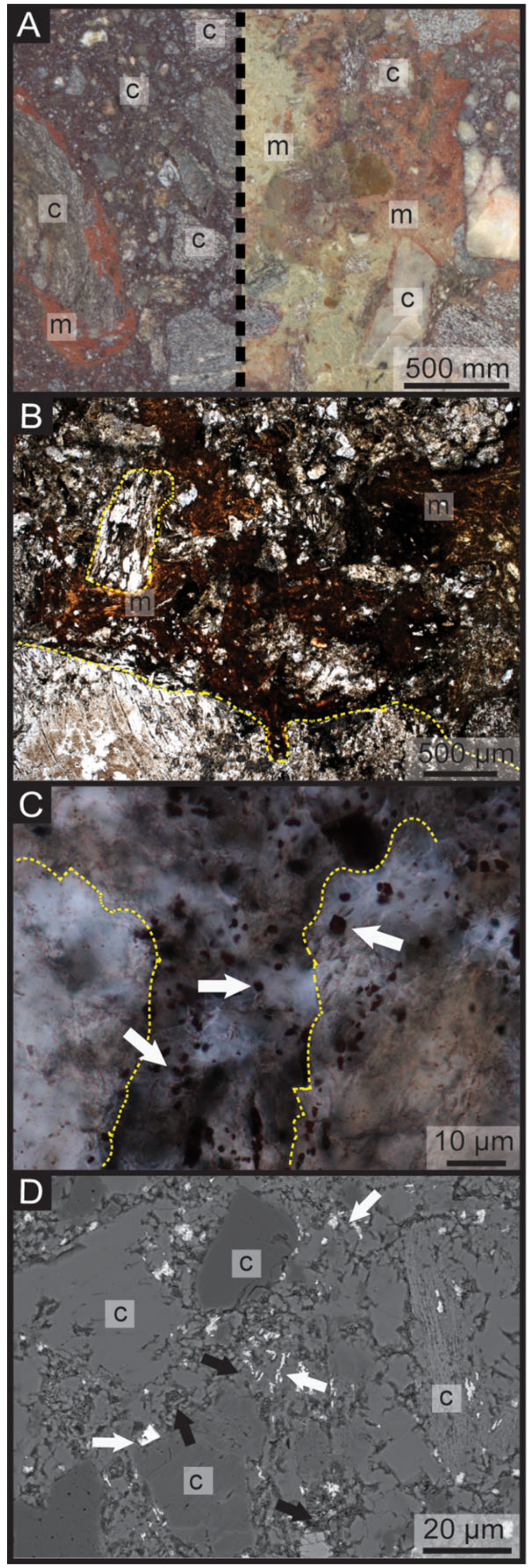

Fig. 4. Unit 3: melt-rich impactite (basal suevite or Valette-type breccias, from Valette). A) Hand sample. Left: low melt content, note the large, highly shocked, and partially melted clast (c) wrapped in reddish melt (m). Right: high melt content. The matrix has a purple hue in contrast to the extensively altered and discolored melt phase. The melt region hosts several subrounded lithic clasts (c). Note also the intricate margins between the melt and the breccia matrix. B, C) Microphotographs. Note the intermingling of the glassy melt phase (m) with the matrix. The melt phase has been altered and appears black and opaque to a translucent yellow-orange. Two large, shocked lithic clasts with irregular, obscure boundaries are outlined. The nature of the interstitial space is ambiguous. Also note the presence of disseminated Ti-Fe oxide grains (white arrows) within the matrix and the similarity of the matrix texture to that of the particulate melt rock (unit 4). D) Backscattered electron (BSE) image. Numerous lithic and mineral clasts (c) are visible in a quartzofeldspathic matrix. Irregular pits (black arrows) are filled with fine-grained clay minerals. It is not clear if these pits represent a preferentially altered phase within a crystalline matrix or altered clasts in a clastic matrix. A secondary Fe-Ti oxide phase (white arrows) is disseminated throughout the matrix and within voids of clasts.

oxhydroxides) are disseminated throughout the matrix (Fig. 4C). At higher magnification under the SEM, the nature of the matrix is somewhat ambiguous. Clast margins are poorly defined and irregular. Interstitial material is poorly resolved.

Numerous subangular lithic and mineral clasts are visible in a quartzofeldspathic matrix with BSE imaging (Fig. 4D). Up to approximately 30% of the matrix is composed of irregular pits filled with fine-grained clay minerals. Glassy, former melt regions have irregular, ameboid margins, and intricate relationships with the matrix. An Fe-Ti oxide phase is disseminated as patchy grains with feathery margins throughout the matrix and within voids in clasts.

Unit 4: ("Montoume Breccia")

Under transmitted light, the unit 4 has a crystalline matrix that varies in color from gray-brown to red (Fig. 5). The matrix commonly displays flow banding that is cross-cut by fractures associated with red-brown discoloration (Figs. 5A and 5B). Flow banding around centimeter sized lithic clasts is also observed in hand specimens (Fig. 5A). This network of fractures and associated discoloration gives the matrix a mesh-like appearance (Fig. 5B). The matrix forms between 10 and 80 vol% of the bulk rock; the remaining material is composed of angular to subangular mineral, lithic, and ameboid glassy clasts (Fig. 5B). Lithic and mineral clasts are dominantly quartz and feldspar, most of them displaying various shock-induced features including planar fractures, PDFs (Fig. 5C), and partial melting. The matrix surrounding the clasts also displays red-brown discoloration due to fine-grained Fe-oxyhydroxides (Fig. 5C). Under high magnification, submicron, red-brown, subhedral crystallites disseminated throughout the

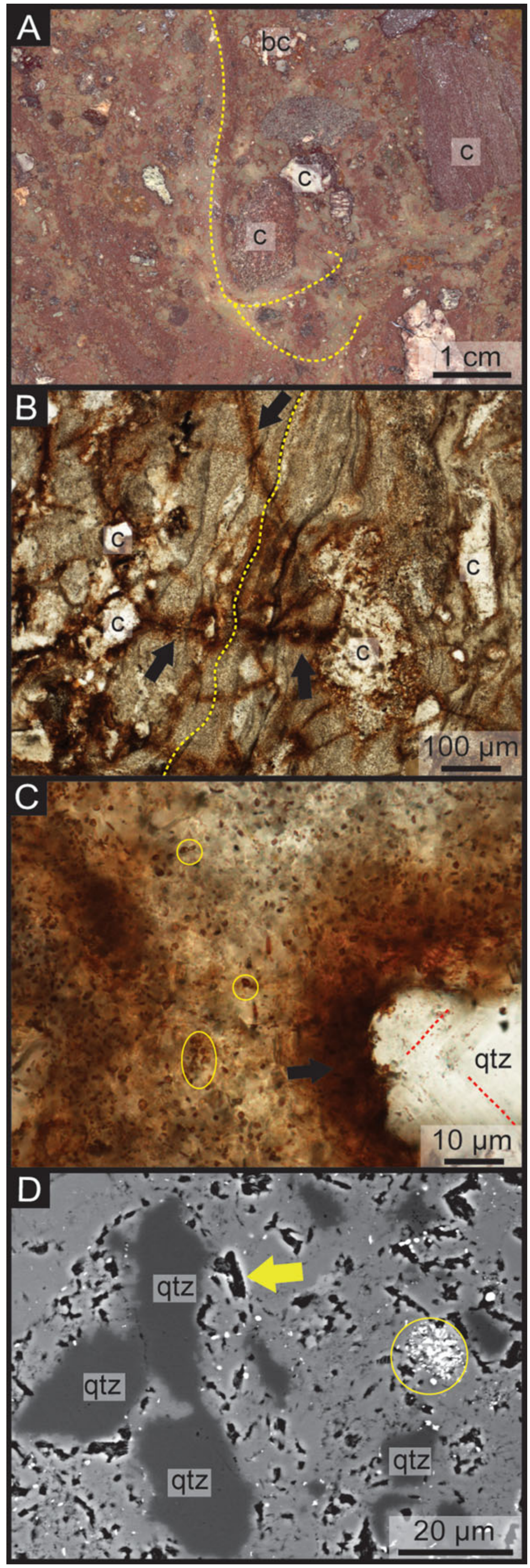

Fig. 5. Unit 4: particulate impact melt (Montoume breccia, from Montoume). A) Hand sample. Note the presence of multiple lithic clasts (c) and one breccia clast (bc). Dashed lines highlight matrix flow features around lithic clasts. B, C) Transmitted light microphotographs. Note the presence of multiple lithic and mineral clasts (c) and a quartz clast (qtz) displaying planar deformation features (dashed lines). Also note the flow banding in the melt matrix (dashed line) and the multiple sets of fractures cross cutting the flow banding (black arrows). The fractures and clasts are associated with rusty discoloration. The discoloration of the fractures formed a mesh-like texture. Also note the red-brown disseminated Fe-Ti oxide grains in the melt matrix circled. D) Backscattered electron (BSE) image. Note the interlocking crystalline nature of the feldspathic matrix. Lath-shaped voids (arrow) are interpreted to represent areas where a mineral phase was completely weathered out. There are many partially resorbed quartz clasts (qtz). The circle encloses a cluster of Fe-Ti oxide grains that are also disseminated throughout the melt.

crystalline matrix, are visible (Fig. 5C). These mineral grains give the matrix a granular texture (Figs. 5B and 5C). Former glassy melt "pockets"/clasts have highly irregular boundaries and commonly fill interstitial spaces within the groundmass.

SEM observations indicate that the matrix has an igneous texture, including interlocking grains of feldspar (Fig. 5D). Lath-shaped pits filled with clay range in size from 25 nm × 1 μm to 2 μm × 25 μm suggesting that one phase of the matrix has been pervasively altered. These pits may make up to 50% of any given area (Fig. 5D). Larger pits have irregular borders, while smaller pits have a more defined lath shape. Other areas are very silica-rich. In these areas the pits make up only approximately 3–5% (area). The margins between the feldspathic and silica-rich areas are highly irregular. The quartz-rich areas may represent a different initial melt phase or large, partially assimilated, quartz grains. There are distinct lithic and mineral grains of millimeter scale throughout the sample. Quartz clasts have complex, undulating margins suggestive of partial assimilation (Fig. 5D). Thread-like strings of Fe-Ti oxide crystals decorate the boundaries between immiscible phases. The distribution of this oxide is heterogeneous; disseminated grains (approximately 10%) appear as isolated rounded grains in the melt ranging from 500 nm to cluster up to approximately 20 μm in size (Ti >>Fe) and as lath shaped (Ti > Fe) approximately 25 nm × 1 μm to clusters up to 5 μm × 15 μm; there are also occasional larger (>100 μm) clusters (Fig. 5D).

Unit 5: ("Babaudus Melt")

In transmitted light, the quartzofeldspathic groundmass of unit 5 is buff colored and has a larger overall grain size (average size of 25 μm) compared to the other impactite units (Fig. 6). The crystalline, vesicular nature of unit 5 is illustrated in Figs. 6B and 6D. Submicron-scale dark crystallites are disseminated in the interlocking, semipolygonal grains, giving the matrix a granular, "sugary" texture (Fig. 6C). The

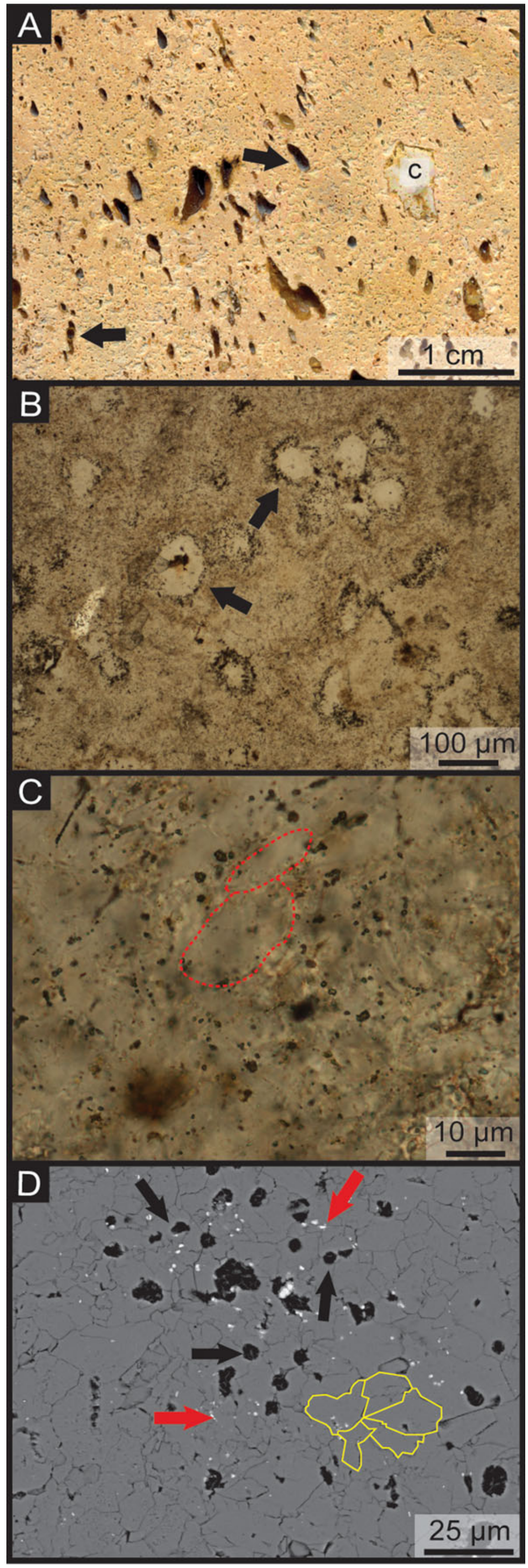

Fig. 6. Unit 5: impact melt rock (Babaudus melt, from Babaudus). A) Hand sample. Note the homogenous nature of the groundmass and numerous slightly elongated vesicles (black arrows). Elongation may be a flow feature. A rare lithic clast (c) with irregular grain boundaries. B, C) Transmitted light photomicrographs: Note the vesicular nature of the melt (B, black arrows) and the igneous texture of interlocking, semipolygonal grains (C, dashed lines). Disseminated Fe-Ti oxide grains give the matrix a speckled texture. D) Backscattered electron (BSE) image: Notice the interlocking sutured grain boundaries indicative of recrystallization (outlined). Black arrows highlight the vesicular nature of the sample. Arrows point to disseminated Fe-Ti oxide grains.

matrix is remarkably homogenous and is mottled with patches of oxide or oxyhydroxide staining (Fig. 6B). The groundmass hosts few clasts in comparison to the other impactite units (Fig. 6A). Lithic clasts are quartzofeldspathic in composition and are generally uniformly small and rounded. Clasts and vesicles are commonly surrounded by alteration halos of iron oxyhydroxide staining. Vesicles are either empty or infilled with fine-grained mineral assemblages. Scanning electron microscopy highlights the presence of interlocking, sutured grain boundaries indicative of recrystallization (Fig. 6D). Micron-scale vesicles are semielliptical in contrast to the centimeter-scale elongated vesicles visible in hand specimen. Submicron iron-titanium nickel-rich oxide grains are disseminated throughout the melt (Fig. 6D).

INTERPRETATIONS AND DISCUSSION

Impactite Nomenclature

Background

Impactite nomenclature and classification has been complicated by ambiguity in the literature (e.g., Reimold et al. 2008). In 1994, the first recommendations for the systematic naming and classification of impactites were proposed (Stöffler and Grieve 1994). Stöffler and Grieve (2007), on the behalf of the IUGS SCMR, published a revised proposal on impactite nomenclature and classification based on texture, degree of shock metamorphism, and lithological components. Reimold et al. (2008) highlighted a number of recent studies that give rise to problems and potential issues with the revised impactite classification scheme. Five specific areas of ambiguity have been identified: (1) field occurrence and confirmation of proposed suevites, (2) scale of impactite classification, (3) marine impactites, (4) transitional lithologies, and (5) pseudotachylitic breccias. With the exception of the identification of possible marine impactites and pseudotachylitic breccias, this paper presents the Rochechouart impactite suite as a case study to address these problematic areas of classification.

One of the most notable discussion points is the application of the term "suevite," which was first used in 1919 to describe a breccia (at that time, interpreted as being volcanic) thought to be unique to the Roman "Provincia Suevia" (Swabia) in Germany (Fraas 1919), at what is now recognized as the Ries impact structure (Pohl et al. 1977). Based on the most recent recommendations of the IUGS SCMR, a "suevite" is an impact breccia with a fine-grained lithic (particulate) matrix hosting both cogenetic lithic and glass clasts. This represents a revision to the original definition of "suevite" by Stöffler et al. (1977) that was defined as a polymict impact breccia with a clastic matrix/groundmass containing fragments and shards of impact glass and shocked mineral and lithic clasts. Unfortunately, the term "suevite" has been used loosely in the literature to refer to any glass-bearing impactite, regardless of groundmass texture (e.g., Kelley and Spray 1997; Masaitis 1999). Indeed, at least three of the impactites studied here—units 2, 3, and 4—have been termed "suevites" in the past based on the IUGS classification scheme, despite the vast differences in appearance, even at the hand specimen scale (Figs. 3–5). As demonstrated in the subsequent section, these impactites also differ in terms of the nature of their groundmass, which is significant with respect to the mode of emplacement. To take into account gradational boundaries and transitional lithologies, a recent subclassification of melt-bearing impactites has been proposed, based on textural analysis of the groundmass or matrix and its relationship with the melt phase(s) and clasts (Osinski et al. 2008).

Classification of the Rochechouart Impactites

High-resolution imaging of the Rochechouart impactites using scanning electron microscopy allowed for detailed observations of textual relationships within, and between, the groundmass and clasts. The Rochechouart impactites have historically been classified based on observable characteristics at the hand sample to thin-section (i.e., optical microscopy) scale and contextual relationships in the field (e.g., Kraut and French 1971; Lambert 1977a). These macro- to intermediate-scale observations are excellent "first principle" classifications and field divisions leading to informal nomenclature. However, as noted above, at the Rochechouart structure, several different "suevite" units have previously been classified, including "basal suevite," "welded suevite," and "upper suevite"; the upper suevite has also been referred to as "Chassenon suevite" and "suevite sensu stricto." The nonuniform use of nomenclature makes it difficult to correlate and compare different studies at this impact structure, let alone between multiple impact structures. Furthermore, the terms "basal" and "upper" are dependent on field relationships between different units. Due to partial erosion at the Rochechouart structure, determining these field relationships is somewhat difficult and in some cases even impossible. Thus, a "suevite" sample with no relative context would not be able to be classified using the current IUGS impactite classification scheme.

A study by Lambert (2010) uses the terminology "suevite sensu stricto" and "melt-rich suevite" to refer to unit 2 and unit 3, respectively. We suggest that this nomenclature be modified and the units classified based on their observable characteristics independent of the connotation of terms such as “suevite” that have been historically misrepresented in the literature. In accordance with the proposed classification schemes of Stöffler and Grieve (2007) modified by Osinski et al. (2008), the following nomenclature is proposed for the Rochechouart impactites (Fig. 7). We suggest that descriptive terminology be used for transitional lithologies where endmember (IUGS) classification cannot distinguish between units such as Rochechouart units 3 through 5.

1. *Unit 1:* lithic (locally monomict to largely polymict) impact breccia, sensu stricto.
2. *Unit 2:* melt-bearing impact breccia (formerly the “Chassenon” or “green” suevite).
3. *Unit 3:* melt-rich impactite. As the primary nature of the groundmass cannot unambiguously be determined, unit 3 cannot be classified as either lithic breccia or impact melt. This unit is a transitional lithology resulting from a continuum between clast-free melt rocks and melt-free lithic impactites.
4. *Unit 4:* particulate impact melt rock; this unit, previously known as the so-called “Montoume breccia,” “red welded breccia/suevite” is clast-rich and has a crystalline, rather than clastic, matrix. As such, this unit is here classified as an impact melt rock.
5. *Unit 5:* impact melt rock; clast-poor to clast-free.

The Rochechouart impactites characterized in this study can be classified as either breccias (units 1 and 2) or melt rocks (units 4 and 5) based on the nature of the groundmass. Unit 3 constitutes a transitional unit between a melt-rich breccia and clast-rich melt rock. While stratigraphic relationships are locally preserved, it is difficult to interpret the spatial extent of the different impactite units due to extensive erosion and concealed fault contacts. Unit 1 overlies shocked target rock and likely formed a continuous sheet overlain by local lenses of unit 2 (cf. Lambert 2010). Preserved outcrops of impact melt lithologies are in contact with the shocked target rock; however, unit 3 is observed at the margins of the exposed remnant of the Valette melt sheet (Lambert 2010). The basal melt sequence is likely transitional in nature, constituting an extension of the continuous breccia sheet (unit 1) in the vicinity of impact melt (units 4 and 5) as observed in the Valette area as local occurrences of unit 3 underlying units 4 and 5.

While the distinction between a lithic breccia and an impact melt-bearing impactite is easily defined by the presence or absence of melt phases (either as clastic or matrix material in a fresh and/or altered state), the textural and genetic relationships between the impact

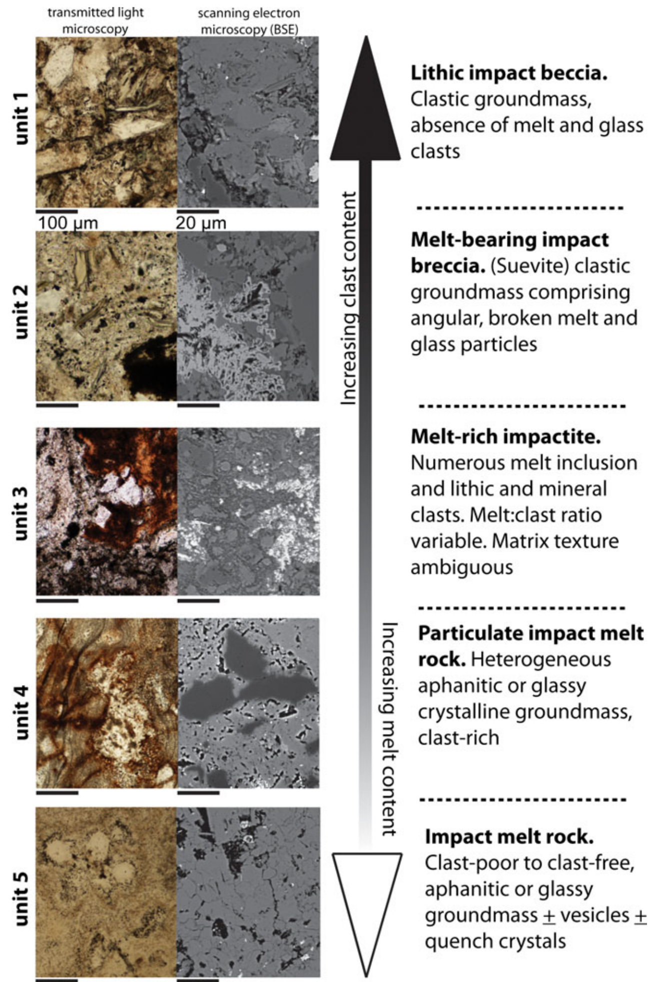

Fig. 7. Descriptive classification of the Rochechouart impactites based on groundmass textures. Note the defining characteristics of each impactite highlighted in the right column text. The images on the left side are representative transmitted light microphotographs and scanning electron images of each unit. Scale bar on all transmitted light micrographs images is 100 µm, scale bar on all scanning electron micrographs is 20 µm.

melt-bearing units (units 2, 3, and 4) are complex. It is only with careful microscopic imagery that characteristic relationships between the matrix and melt phases can be elucidated. As noted by Osinski et al. (2004) and exemplified here by units 3 and 4, care should be exercised when interpreting seemingly “clastic” textures based on hand specimen and optical studies alone. Unit 2, corresponding to the classic “Chassenon suevite” or “upper suevite” of Lambert (2010) likely represents a lithology in the continuum between impact melt-free and melt-rich impactites. The impact melt-rich impactite (unit 3; previously “basal suevite”) is highly variable in composition and texture.

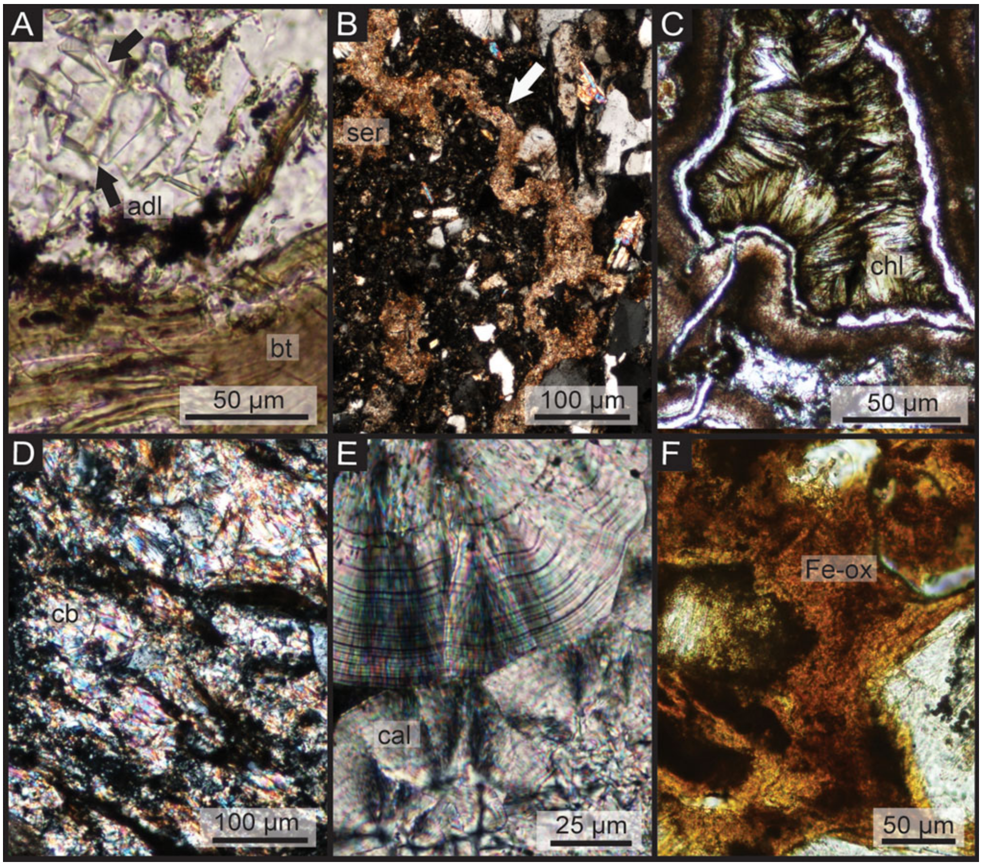

Fig. 8. Alteration mineral assemblages in the Rochechouart impactites. A) Subhedral to euhedral adularia rhombs (black arrows), plane-polarized light micrograph. Unit 2, melt-bearing impact breccia. B) Seritic alteration in a fracture between two clasts (white arrow), crossed polarized light micrograph. Unit 1, lithic impact breccia. C) Amygdaloidal chlorite, plane-polarized light micrograph. Unit 2, melt-bearing impact breccia. D) Pervasive carbonate alteration, crossed polarized light micrograph. Unit 2, melt-bearing impact breccia. E) Banded calcite within a void space, crossed polarized light micrograph. Unit 1, lithic impact breccia. F) Iron-oxide staining, plane-polarized light micrograph. Unit 5, impact melt rock. adl = adularia, bt = biotite, cal = calcite, cb = carbonate, chl = chlorite, Fe-ox = iron oxides, ser = sericite.

This impact melt-rich unit is located in direct contact with the basement rocks and always in close proximity to the particulate impact melt rocks (Lambert 2010). The matrix, formerly reported as clastic, incorporates up to 50 vol% melt clasts (Lambert 2010). We cannot definitively classify the matrix as either clastic or crystalline as extensive postimpact hydrothermal alteration obscures the primary texture (Figs. 4C and 4D). The matrix is very similar in texture and composition, as assessed by EDX analyses, to that of unit 4 (particulate clast-rich impact melt rock). The characteristics of this melt-rich impactite do not conform to the definition of suevite sensu stricto and should not be termed as such. Unit 3 is both texturally and genetically transitional between the polymict lithic breccia and particulate melt rock, as proposed and discussed by Lambert (2010) and as such we have classified unit 3 as a transitional unit overlying shocked target rock and overlain by impact melt rock.

Complications Due to Weathering and Alteration

Impactite lithologies were subject to complex alteration processes as noted above. Weathering and alteration led to the formation of secondary and even tertiary mineral phases that overprint primary textures and mineralogy (Fig. 8). For example, chloritization (Figs. 2B and 7C) and argillic clay alteration often completely replace feldspar grains in the Rochechouart impact breccias. The matrix of the impact melt-rich impactite (unit 3) contains numerous "pits" filled with fine-grained clay minerals. It is not clear if these patches of clay represent a mineral phase within a crystalline matrix that has been preferentially altered (as in the crystalline impact melt rock), or altered fine-grained material interstitial to larger clasts within a cataclastic matrix. Such an extensive alteration, as with the examples presented above, leads to difficulties assigning primary mineralogy and even in some cases primary textures. Impact glasses may be partially or completely devitrified, resulting in a mixture of clay minerals, and Fe-Ti oxides, or weathered out completely, leaving a vesicular-like texture to glass-bearing impact breccias. The alteration along fractures and of surrounding clasts in the particulate clast-rich impact melt rock is suggestive of hydrous alteration. SEM imaging can elucidate the complex relationships between clasts and the matrix and potentially deconvolve the overprinting signatures of weathering, postimpact hydrothermal activity, and regional metamorphism. The extensive alteration resulting from devitrification, postimpact hydrothermal activity, and terrestrial weathering processes underscores the importance of detailed microscale observations.

Impact-Generated Hydrothermal Activity at Rochechouart

Alteration of the Rochechouart impactites has been previously noted by several researchers (Kraut and French 1971; Lambert 1977b, 1977c; Reimold 1987); however, the postimpact hydrothermal system has not been described in any detail in previous studies. We recognize three main alteration assemblages (1) potassic argillic-like (adularia (Fig. 8A), smectite clays, chlorite (Fig. 8C), sericite (Fig. 8B); (2) carbonate (Fig. 8D) (calcite [Fig. 8E]); and (3) oxide (Fig 8F), possibly reflecting differing alteration conditions and heterogeneous primary material. The dominant K-rich clay mineralization alteration assemblage at Rochechouart is consistent with the general patterns of postimpact hydrothermal systems discussed by Naumov (2005) and Naumov et al. (2002). The alteration assemblages are present in both allochthonous and autochthonous impactites, but are most prevalent in units 3 and 5.

The intense evidence of K-metasomatism in all impactite units is indicative of pervasive, deep-circulation of hydrothermal fluids (Lambert 1977c, 2010; Schmieder et al. 2010). All impactite units have K_2O/Na_2O ratios greater than 1 (Lambert 1977c). Interestingly, this K enrichment systematically increases with melt content. The K_2O/Na_2O ratios of the lithic polymict breccia is approximately five times that of the unshocked basement rocks, approximately six times higher in suevite, approximately ten times higher in lithic clasts within melt rocks, and approximately fifteen times higher in melt (Lambert 1977c, 2010). The pervasive argillic-like alteration assemblages, together with fine-grained quartz and carbonate mineralization, are consistent with the development of a postimpact hydrothermal system (e.g., Naumov 2005; Osinski et al. 2013), as previously suggested by Reimold and Oskierski (1987). Staining by alteration products is most prevalent in oxide-rich units, such as in the hematite-rich particulate melt rock (unit 3). However, it is still unclear why the melt phases in the particulate melt rock are richer in oxides than the crystalline melt.

It is notable that the accessory phases present in the impactite units vary with the impact melt content. Both the lithic breccia and melt-bearing breccias contain rounded, embayed apatite grains. Apatite was not seen in the particulate clast-rich melt or crystalline melt units. It is interesting to note that apatite is unstable in the presence of Cl-rich fluids (Boudreau et al. 1986). The correlation between K_2O/Na_2O ratios and the presence of melt suggests that hydrothermal alteration was more intense in these units, possibly resulting in apatite recrystallization. In contrast, oxides and oxyhydroxides are more prevalent in the melt-rich units. This may be a consequence of homogenization and immiscibility between phases at a local scale. Oxides also commonly form skeletal quench textures within the silicate melt, thus, there is likely three generations of oxides (1) primary relict accessory mineral oxides from the target rock occurring in the melt-free impactites, (2) impact-generated oxides forming quench crystallites within the melt, and (3) oxide staining as a result of postimpact alteration processes.

Implications for the Rochechouart Impact Structure

Comparison With Other Craters in Crystalline Targets

A major question for the Rochechouart structure is why does there not appear to be a "simple" relatively clast-free impact melt sheet? Studies of other midsized complex impact structures developed in crystalline targets—such as the 24 km diameter Boltysh (Grieve et al. 1987), the approximately 26 km diameter and ≥36 km diameter East and West Clearwater Lakes (Simonds et al. 1978b), and the 28 km diameter Mistastin (Grieve 1975) impact structures—and considerations of the origin and emplacement of impact melts (Grieve et al. 1977; Osinski et al. 2008) would suggest that this should be the case. The reclassification of impactites proposed herein goes part way to answering this question, but uncertainty remains. As an example, the well-preserved 24 km Boltysh impact structure, Ukraine (Grieve et al. 1987), which formed in the crystalline Precambrian basement of the Ukrainian shield, shares a similar stratigraphic sequence of impactites to that proposed here for Rochechouart. The approximately 200 m thick Boltysh impact melt sheet lies directly over polymict lithic breccias of the crater floor and is overlain by approximately 25 m of "suevitic breccia" (Grieve et al. 1987; Williams 2012). This melt sheet contains approximately 10% granitic clasts displaying varying degrees of assimilation (Grieve et al.

1987). It is also of note that the top approximately 60 m of the Boltysh melt unit is described as a clast-poor microcrystalline impact melt (Grieve et al. 1987), which is similar to the aphanitic vesicular impact melt at Rochechouart (unit 5). Thus, we suggest that the clast-poor aphanitic vesicular impact melt rock (unit 5) may have occurred as scattered, isolated lenses within and/or near the top of the impact melt "sheet" or that these outcrops represent melt near the crater center.

We suggest that the textural and chemical properties, together with the stratigraphic relations, of the Rochechouart impactites, are consistent with the particulate clast-rich impact melt rock (unit 4) being the main allochthonous crater-fill unit, equivalent to the coherent impact melt sheets observed in impact structures such as Mistastin (Grieve 1975). This is supported by the presence of columnar joints that are clearly visible in the Montoume quarry. Similar columnar jointing in impactites has only been observed in impact melt sheets, such as at the Mistastin (Grieve 1975) and Manicouagan (Simonds et al. 1978a) impact structures (both in Canada). However, it is unclear as to why the clast content of the main Rochechouart melt sheet (interpreted here to be the clast-rich melt rock) is so high, although the partial erosion of Rochechouart may be a factor in that we may only be viewing the basal sequence of the original melt sheet.

Location of the Crater Center and Size of the Rochechouart Structure

The above discussions have potential implications for determining the center of the Rochechouart impact structure and, correspondingly, its size. Previous work (Kraut and French 1971; Lambert 1974, 1977b) estimates the crater center to be in the Valette area (Fig. 1), based on the distribution of the impact breccias/impact melt rocks and on the distribution and orientation of shatter cones. It has since been shown that the distribution and orientation of shatter cones is an inherently unreliable method to determine the center of an impact structure (Osinski and Spray 2006; Wieland et al. 2006). In addition, if unit 3 (i.e., melt-rich impactite) represents the main crater-fill material, then, the center of the crater may be approximately 6 km farther to the south, near the village of Montoume (Fig. 1). The Montoume quarry hosts a 900 m long, 600 m wide, and 25 m high outcrop of the particulate impact melt lithology (unit 4) and is the thickest known sequence of impact melt material at the scale of the whole structure. Moving the crater center to the south would place the main outcropping area of unit 5 (i.e., at Chassenon; Fig. 1), in the crater rim area—if the crater diameter remains the same (i.e., 24 km). However, a few shatter cone occurrences are known in the Chassenon area (e.g., Lambert 1977a, 2010), and were recently confirmed during a mapping campaign of the distribution of shatter cone at the Rochechouart structure by one of the authors (L.F.). If these occurrences of shatter cones are truly in situ, then this would be inconsistent with placing Chassenon in the crater rim area. Invoking a larger crater diameter is one possible solution. Thus, if the size for the proposed crater diameter is increased and the crater center placed farther south, near the village of Montoume, then the Chassenon area would be well inside the original crater rim, consistent with the recent mapping of shatter cone distribution. A crater diameter in the 40–50 km range has been suggested by studying topographic comparisons using crater profile data of Rochechouart with other structures, including the Ries and the El'gygytgyn impact structures (Lambert 2010). More conclusive data is required to support this suggestion but a diameter in this range certainly seems possible from the results of our study, in particular if the particulate clast-rich impact melt rock is a small remnant of the basal parts of a once much more extensive and thicker crater-fill impact melt sheet.

Finally, we note that the distribution of impactites and shock indicators may be biased in the northern part of the structure as the crater floor is inclined 0.6° to the north (Lambert 1977a, 2010). Such an inclination of 0.6° over a 24 km lateral distance corresponds to an approximate vertical difference of 250 m between the northern and southern extents of the structure. This inclination may have led to preferential erosion of impactite outcrops south of the structure, as the present-day erosional level is approximately equal to the crater floor. Such asymmetrical erosion could have led to the preservation of stratigraphically higher impactite units to the northern part such as impact melt-bearing breccias and an impactoclastic unit and resulted in the erosion of ejecta deposits.

The Rhaetian determination of approximately 203 Ma for the Rochechouart impact structure has raised speculation regarding a possible impact component to the Triassic–Jurassic mass extinction event. The importance of the link between meteorite impacts and Earth evolution finally entered the geological mainstream in the 1980s, with evidence for a major impact as the cause of the mass extinction event at the Cretaceous–Palaeogene (K–Pg) boundary approximately 66 Myr ago (Alvarez et al. 1980; Renne et al. 2013). The actual impact site, the approximately 180 km diameter Chicxulub crater, was subsequently identified in 1991, buried beneath approximately 1 km of sediments in the Yucatan peninsula, Mexico

(Hildebrand et al. 1991). Despite some controversy, it is apparent that the Chicxulub impact event and its aftermath account for the sudden extinctions at the K–Pg boundary (Schulte et al. 2010). This remains, to date, the only unambiguous association of an impact event and crater with a mass extinction event in the geological record. First suspected following the discovery of a complex iridium anomaly at and slightly below the stratigraphic Triassic/Jurassic boundary (Olsen et al. 2002) the correspondence between the age of the Triassic–Jurassic boundary and the new reported age for the Rochechouart impact structure (Schmieder et al. 2009a, 2009b, 2010; Smith 2011) has been noted. The eroded nature of this site complicates reconstruction of the original impact crater. We suggest that the Rochechouart crater diameter may have been in the 40–50 km range consistent with estimations of Lambert (2010). It is generally considered that an impact in the 20–30 km size range would be unlikely to cause any significant global environmental perturbations (e.g., Pierazzo and Artemieva 2012). Thus, either multiple impacts would need to be involved or the impact-hypothesis for the T–J mass extinction of Olsen et al. (2002) must be reexamined in the context of Rochechouart.

CLOSING REMARKS

High-resolution imaging of the Rochechouart impactites using scanning electron microscopy combined with optical microscope observations has enabled elucidation of textual relationships within, and between, the groundmass and clasts. In summary, groundmass textures form a continuum largely based on the proportion of impact melt (glass and crystallites) between the aphanitic crystalline matrix of the clast-poor to clast-free impact melt rock (unit 5) and the fragmental, clastic matrix of the melt-free lithic breccia (unit 1). This study of the Rochechouart impactites underscores the importance of establishing consistent use of nomenclature in the literature.

The classification system applied to the Rochechouart impactites in this study allows for gradational lithologies in addition to being beneficial for samples/sites with limited exposure and little to no field context. Developing such a system and applying it to all impact structures will allow correlation between sites and studies as well as set a precedent for limited sample environments (e.g., Ritland impact structure; Riis et al. 2011). It is hoped that this type of “multiscale” classification of impactites will allow correlations between impact structures in very different target lithologies, as the impactite nomenclature is independent of relationships between impactite lithologies and relationships between lithologies and the impact structure itself.

It is hoped that these new observations will stimulate renewed interest in the study of the Rochechouart impact structure. Despite its location in Western Europe, the Rochechouart impact structure has been relatively little studied especially compared to its close neighbor, the Ries impact structure in Germany. As we have shown here, erosion hampers our understanding of this structure, but important new observations and interpretations can still be made. The potential larger diameter of the Rochechouart structure, in the range of 40–50 km, is supported by our study, would definitely have affected a much larger area than previously thought and likely induced regional or even global environmental perturbations.

Acknowledgments—This research was funded by Natural Sciences and Engineering Council of Canada (NSERC) Discovery Grants to GRO and NB the Canadian Space Agency’s (CSA) Canadian Analogue Research Network (CARN). GRO is supported by an NSERC/MDA/CSA Industrial Research Chair in Planetary Geology. Ivan Barker (UWO ZAPLab), Callum Hetherington and Mark Grimson (Texas Tech), and Todd Simpson (UWO Nanofabrication laboratory) are thanked for technical assistance with the SEM measurements. We thank the Rochechouart museum for providing us samples 42 and 43. This paper is dedicated to the memory of François Kraut (1907–1983), who first described the Rochechouart breccias as impactites.

The authors declare that there are no real or perceived potential sources of conflict of interest. There are no interests or relationships, financial or otherwise, that might be perceived as influencing an author’s objectivity relevant or indirectly related to the work described in this manuscript.

Editorial Handling—Dr. A. J. Timothy Jull

REFERENCES

Alvarez L. W., Alvarez W., Asaro F., and Michel H. V. 1980. Extraterrestrial cause for the Cretaceous/Tertiary extinction. *Science* 208:1095–1108.

Boudreau A. E., Mathez E. A., and McCallum I. S. 1986. Halogen geochemistry of the Stillwater and Bushveld complexes; evidence for transport of the platinum-group elements by Cl-rich fluids. *Journal of Petrology* 27:967–986.

Cohen K. M., Finney S. M., Gibbard P. L., and Fan J.-X. 2013. The ICS International Chronostratigraphic Chart. *Episodes* 363:199–204.

Ferrière L., Koeberl C., and Reimold W. U. 2009a. Characterization of ballen quartz and cristobalite in impact breccias: New observations and constraints on ballen formation. *European Journal of Mineralogy* 21:203–217.

Ferrière L., Koeberl C., Reimold W. U., Hect L., and Bartosova K. 2009b. The origin of "toasted" quartz in impactites revisited (abstract #1751). 40th Lunar and Planetary Science Conference. CD-ROM.

Ferrière L., Koeberl C., Libowitzky E., Reimold W. U., Greshake A., and Brandstätter F. 2010. Ballen quartz and cristobalite in impactites: New investigations. In *Large meteorite impacts and planetary evolution IV*, edited by Gibson R. L. and Reimold W. U. GSA Special Paper 465. Boulder, Colorado: Geological Society of America. pp. 609–618.

Fraas E. 1919. Begleitworte zu der geognostischen Spezialkarte von Württemberg—Atlasblatt Bopfingen. Statistisches Landesamt, Kohlhammer, Stuttgart, Germany. 31 p. (In German).

Grieve R. A. F. 1975. Petrology and chemistry of impact melt at Mistastin Lake Crater, Labrador. *Geological Society of America Bulletin* 86:1617–1629.

Grieve R. A. F., Dence M. R., and Robertson P. B. 1977. Cratering processes—As interpreted from the occurrence of impact melts. In *Impact and explosion cratering; planetary and terrestrial implications*, edited by Roddy D. J., Pepin R. O., and Merrill R. B. Proceedings of the Symposium on planetary cratering mechanics. New York: Pergamon Press. pp. 791–814.

Grieve R. A. F., Reny G., Gurov E. P., and Ryabenko V. A. 1987. The melt rocks of the Boltysh Impact Crater, Ukraine, USSR. *Contributions to Mineralogy and Petrology* 96:56–62.

Hildebrand A. R., Penfield G. T., Kring D. A., Pilkington M., Camargo A., Jacobsen S. B., and Boynton W. V. 1991. Chicxulub crater—A possible cretaceous tertiary boundary impact crater on the Yucatan Peninsula, Mexico. *Geology* 19:867–871.

Jourdan F., Reimold W. U., and Deutsch A. 2012. Dating terrestrial impact structures. *Elements* 8:49–53.

Kelley S. P. and Spray J. G. 1997. A Late Triassic age for the Rochechouart impact structure, France. *Meteoritics & Planetary Science* 32:629–636.

Kraut F. 1967. Sur l'origine des clivages du quartz dans les brèches "volcaniques" de la région de Rochechouart. *Comptes-Rendus de l'Académie des Sciences de Paris* 264:2609–2612.

Kraut F. 1969. Über ein neues Impaktit-Vorkommen im Gebiete von Rochechouart-Chassenon. *Geologica Bavarica* 61:428–450.

Kraut F. and French B. M. 1971. The Rochechouart meteorite impact structure, France; preliminary geological results. *Journal of Geophysical Research* 76:5407–5413.

Kraut F., Short N. M., and French B. M. 1969. Preliminary report on a probable meteorite impact structure near Chassenon, France. *Meteoritics* 4:190–191.

Lambert P. 1974. Etude géologique de la structure impactitique de Rochechouart (Limousin, France) et son contexte [A geologic study of the impactite structure of Rochechouart (Limousin, France) and its context]. *Bulletin du Bureau de Recherches Géologiques et Minières. Section 1: Géologie de la France* 3:153–164.

Lambert P. 1977a. Les effets des ondes de choc naturelles et artificielles, et la cratère d'impact de Rochechouart (LimousinFrance). Ph.D. thesis, Université de Paris-Sud, Centre d'Orsay, France.

Lambert P. 1977b. Rochechouart impact crater; statistical geochemical investigations and meteoritic contamination; Impact and explosion cratering; planetary and terrestrial implications. In *Impact and explosion cratering; planetary and terrestrial implications*, edited by Roddy D. J., Pepin R. O., and Merrill R. B. Proceedings of the Symposium on planetary cratering mechanics. New York: Pergamon Press. pp. 449–460.

Lambert P. 1977c. The Rochechouart Crater; shock zoning study. *Earth and Planetary Science Letters* 35:258–268.

Lambert P. 1982. Rochechouart: A flag crater from a clustered impact. *Meteoritics* 17:240–241.

Lambert P. 2010. Target and impact deposits at Rochechouart impact structure, France. In: *Large meteorite impacts and planetary evolution IV*, edited by Gibson R. L. and Reimold W. U. GSA Special Paper 465. Boulder, Colorado: Geological Society of America. pp. 509–541.

Masaitis V. L. 1999. Impact structures of northeastern Eurasia: The territories of Russia and adjacent countries. *Meteoritics & Planetary Science* 34:691–711.

Naumov M. V. 2005. Principal features of impact-generated hydrothermal circulation systems: Mineralogical and geochemical evidence. *Geofluids* 5:165–184.

Naumov M. V., Plado J., and Pesonen L. J. 2002. Impact-generated hydrothermal systems; data from Popigai, Kara, and Puchezh-Katunki impact structures. In *Impacts in Precambrian shields*, edited by Koeberl C. Berlin: Springer. pp. 117–171.

Nelson M. J., Newsom H. E., Spilde M. N., and Salge T. 2012. Petrographic investigation of melt and matrix relationships in Chicxulub crater Yaxcopoil-1 brecciated melt rock and melt rock-bearing suevite (846–885 m, units 4 and 5). *Geochimica et Cosmochimica Acta* 86:1–20.

Olsen P. E., Kent D. V., Sues H. D., Koeberl C., Huber H., Montanari A., Rainforth E. C., Fowell S. J., Szajna M. J., and Hartline B. W. 2002. Ascent of dinosaurs linked to an iridium anomaly at the Triassic-Jurassic Boundary. *Science* 296:1305–1307.

Osinski G. R. and Spray J. G. 2001. Impact-generated carbonate melts: Evidence from the Haughton structure, Canada. *Earth and Planetary Science Letters* 194:17–29.

Osinski G. R. and Spray J. G. 2006. Shatter cones of the Haughton impact structure, Canada, Proceedings of the 1st International Conference on the Impact Cratering in the Solar System. European Space Agency Special Publication SP-612 (CD-ROM).

Osinski G. R., Grieve R. A. F., and Spray J. G. 2004. The nature of the groundmass of surficial suevite from the Ries impact structure, Germany, and constraints on its origin. *Meteoritics & Planetary Science* 39:1655–1683.

Osinski G. R., Grieve R. A. F., Collins G. S., Marion C., and Sylvester P. 2008. The effect of target lithology on the products of impact melting. *Meteoritics & Planetary Science* 43:1–45.

Osinski G. R., Tornabene L. L., Banerjee N. R., Cockell C. S., Flemming R. L., Izawa M. R. M., McCutcheon J., Parnell J., Preston L. J., Pickersgill A. E., Pontefract A., Sapers H. M., and Southam G. 2013. Impact-generated hydrothermal systems on Earth and Mars. *Icarus* 224:347–363.

Pierazzo E., and Artemieva N. A. 2012. Local and global environmental effects of impacts on Earth. *Elements* 8:55–60.

Pohl J., Stöffler D., Gall H., and Ernstson K. 1977. The Ries impact crater. In *Impact and explosion cratering; planetary and terrestrial implications*, edited by Roddy D. J., Pepin R. O., and Merrill R. B. Proceedings of the Symposium on planetary cratering mechanics. New York: Pergamon Press. pp. 343–404.

Pohl J., Ernstson K., and Lambert P. 1978. Gravity measurements in the Rochechouart impact structure (France). *Meteoritics* 13:601–604.

Reimold W. U. 1987. The pseudotachylite from Champagnac in the Rochechouart meteorite crater, France. *Journal of Geophysical Research* 92:E737–E748.

Reimold W. U., and Oskierski W. 1987. The Rb-Sr-age of the Rochechouart impact structure, France, and geochemical constraints on impact melt-target rock-meteorite compositions. In *Research in terrestrial impact structures*, edited by Pohl J. Braunschweig: Vieweg & Sohn. pp. 94–114.

Reimold W. U., Horton J. W. Jr., and Schmitt R. T. 2008. Debate about impactite nomenclature—Recent problems (abstract #3033). In *Large meteorite impacts and planetary evolution IV*. LPI Contribution No. 1423. Houston, Texas: Lunar and Planetary Institute. pp. 187–188.

Renne P. R., Mundil R., Balco G., Min K., and Ludwig K. R. 2010. Joint determination of ^{40}K decay constants and ^{40}Ar*/^{40}K for the Fish Canyon sanidine standard, and improved accuracy for ^{40}Ar/^{39}Ar geochronology. *Geochimica et Cosmochimica Acta* 74:5349–5367.

Renne P. R., Balco G., Ludwig K. R., Mundil R., and Min K. 2011. Response to the comment by W. H. Schwarz et al. on "Joint determination of ^{40}K decay constants and ^{40}Ar/^{40}K for the Fish Canyon sanidine standard, and improved accuracy for ^{40}Ar/^{39}Ar geochronology by P. R. Renne et al., 2010." *Geochimica et Cosmochimica Acta* 75:5097–5100.

Renne P. R., Deino A. L., Hilgen F. J., Kuiper K. F., Mark D. F., Mitchell W. S., Morgan L. E., Mundil R., and Smit J. 2013. Time scales of critical events around the Cretaceous-Paleogene boundary. *Science* 339:684–687.

Riis F., Kalleson E., Dypvik H., Krøgli S. O., and Nilsen O. 2011. The Ritland impact structure, southwestern Norway. *Meteoritics & Planetary Science* 46:748–761.

Schmieder M., Buchner E., Schwarz W. H., Trieloff M., and Lambert P. 2009a. A Triassic/Jurassic boundary age for the Rochechouart impact structure (France) (abstract #5138). *Meteoritics & Planetary Science* 44:A186.

Schmieder M., Lambert P., and Buchner E. 2009b. Did the Rochechouart impact (France) trigger an end-Triassic tsunami? (abstract #5140). *Meteoritics & Planetary Science* 44:A186.

Schmieder M., Buchner E., Schwarz W. H., Trieloff M., and Lambert P. 2010. A Rhaetian ^{40}Ar/^{39}Ar age for the Rochechouart impact structure (France) and implications for the latest Triassic sedimentary record. *Meteoritics & Planetary Science* 45:1225–1242.

Schulte P., Alegret L., Arenillas I., Arz J. A., Barton P. J., Bown P. R., Bralower T. J., Christeson G. L., Claeys P., Cockell C. S., Collins G. S., Deutsch A., Goldin T. J., Goto K., Grajales-Nishimura J. M., Grieve R. A. F., Gulick S. P. S., Johnson K. R., Kiessling W., Koeberl C., Kring D. A., MacLeod K. G., Matsui T., Melosh J., Montanari A., Morgan J. V., Neal C. R., Nichols D. J., Norris R. D., Pierazzo E., Ravizza G., Rebolledo-Vieyra M., Reimold W. U., Robin E., Salge T., Speijer R. P., Sweet A. R., Urrutia-Fucugauchi J., Vajda V., Whalen M. T., and Willumsen P. S. 2010. The Chicxulub asteroid impact and mass extinction at the Cretaceous-Paleogene boundary. *Science* 327:1214–1218.

Simonds C. H., Floran R. J., McGee P. E., Phinney W. C., and Warner J. L. 1978a. Petrogenesis of melt rocks, Manicouagan impact structure, Quebec. *Journal of Geophysics Research* 83:2773–2778.

Simonds C. H., Phinney W. C., McGee P. E., and Cochran A. 1978b. West Clearwater, Quebec impact structure, Part I: Field geology, structure and bulk chemistry. Proceedings, 9th Lunar and Planetary Science Conference. pp. 2633–2658.

Smith R. 2011. Dark days of the Triassic: Lost world. *Nature* 479:287–289.

Stöffler D. and Grieve R. A. F. 1994. Classification and nomenclature of impact metamorphic rocks; a proposal to the IUGS subcommission on the systematics of metamorphic rocks. Proceedings, 25th Lunar and Planetary Science Conference. Part 3. p. 1347.

Stöffler D. and Grieve R. A. F. 2007. Classification and nomenclature scheme; impactites modified. In *Metamorphic rocks, a classification and glossary of terms; recommendations of the International Union of Geological Sciences Subcommission on the Systematics of Metamorphic Rocks*, edited by Fettes D. and Desmons J. Cambridge: Cambridge University Press. pp. 82–92.

Stöffler D., Ewald U., Ostertag R., and Reimold W. U. 1977. Research drilling Nöördlingen 1973 (Ries): Composition and texture of polymict impact breccias. *Geologica Bavaria* 75:163–189.

Turpin L., Cuney M., Friedrich M., Bouchez J. L., and Aubertin M. 1990. Meta-igneous origin of Hercynian peraluminous granites in N. W. French Massif Central; implications for crustal history reconstructions. *Contributions to Mineralology and Petrology* 104:163–172.

Whitehead J., Spray J. G., and Grieve R. A. F. 2002. Origin of "toasted" quartz in terrestrial impact structures. *Geology* 30:431–434.

Wieland F., Reimold W. U., and Gibson R. L. 2006. New observations on shatter cones in the Vredefort impact structure, South Africa, and evaluation of current hypotheses for shatter cone formation. *Meteoritics & Planetary Science* 41:1737–1759.

Williams F. A. 2012. Variations through the Boltysh suevites: Glasses, groundmass and hydrothermal minerals (abstract #5077). *Meteoritics & Planetary Science* 47.